6-*d* isotopomers; 2-methyl-*endo*-2-bicyclo[2.2.1]heptanol and its methyl-d_3 and 3,3-d_2 isotopomers; 2-cyclopropyl-2-propanol and the 1,1,1,3,3,3-d_6 isotopomer; and 2-methyl-2-adamantanol and the methyl-d_3 isotopomer. Alcohols were purified by dry column flash chromatography using Merck silica gel 60 (finer than 230 mesh) or preparative gas chromatography on a 6-m column packed with 5% Carbowax on 80/100 mesh Chromosorb W High Pack. Chlorides were prepared by the procedure of Brown et al.[34] or the procedure of Norris and Olmstead[35] and were used without further purification.

Bicyclo[2.2.2]octan-2-one-*3,3-d*$_2$ and bicyclco[2.2.1]heptan-2-one-*3,3-d*$_2$ were prepared as previously described.[36] Cyclopropyl methyl-d_3 ketone was obtained by three repetitions of base-catalyzed (K_2CO_3) exchanges of cyclopropyl methyl ketone in D_2O as 55-60 °C for 15 h.

Bicyclo[2.2.2]octan-2-one-*6-d* was prepared by the sequence shown in Scheme I. The Diels-Alder reaction[37] of 2-((trimethylsilyl)oxy)-1,3-cyclohexadiene[36] with acrylonitrile in toluene at 140 °C for 48 h afforded 2-cyano-5-((trimethylsilyl)oxy)-5-bicyclo[2.2.2]octene in 92% yield. Methanolysis of the silyl enol ether with CH_3OD catalyzed by $NaOCH_3$ gave 5-cyanobicyclo[2.2.2]octan-2-one-*2,2-d*$_2$ in 78% yield. Conversion to the tosylhydrazone in ethanol (substantial loss of deuterium occurred here) and reduction[38] gave 2-cyanobicyclo[2.2.2]octane-*6-d* in 66% yield. Conversion to bicyclo[2.2.2]octan-2-one-*6-d* was accomplished by chlorination and hydrolysis in the method of Freeman et al.[37]

Acknowledgment. Partial financial support for this research was provided by the National Science Foundation (Grant CHE-8211125).

Registry No. 1, 66344-74-9; **2**, 3197-78-2; **4**, 27411-03-6; **5**, 25681-56-5; D_2, 7782-39-0; bicyclo[2.2.2]octan-2-one-*6-d*, 110773-20-1; 2-cyano-5-((trimethylsilyl)oxy)-5-bicyclo[2.2.2]octene, 110773-21-2; 5-cyanobicyclo[2.2.2]octan-2-one-*3,3-d*$_2$, 110773-22-3; 2-cyanobicyclo-[2.2.2]octane-*6-d*, 110773-23-4; 2-((trimethylsilyl)oxy)-1,3-cyclohexadiene, 54781-19-0; 2-methyl-6-deuteriobicyclo[2.2.2]octan-2-ol, 110773-24-5; 2-chloro-6-deuterio-2-methylbicyclo[2.2.2]octane, 110773-25-6.

(34) Brown, H.; Rei, M. *J. Org. Chem.* **1966**, *31*, 1090.
(35) Norris, J. F.; Olmsted, A. W. *Org. Synth.* **1941**, *Collect. Vol. 1*, 144.
(36) Forsyth, D. A.; Botkin, J. H.; Osterman, V. M. *J. Am. Chem. Soc.* **1984**, *106*, 7663.
(37) Freeman, P. K.; Balls, D. M.; Brown, D. J. *J. Org. Chem.* **1968**, *33*, 2211.
(38) Hutchins, R. D.; Maryanoff, B. E.; Milewski, C. A. *J. Am. Chem. Soc.* **1971**, *93*, 1793.

Self-Diffusion Coefficients of Solvents in Polystyrene Gels

Warren T. Ford,*† Bruce J. Ackerson,‡ Frank D. Blum,§ M. Periyasamy,† and Stephen Pickup§

Contribution from the Departments of Chemistry and Physics, Oklahoma State University, Stillwater, Oklahoma 74078, and the Department of Chemistry, Drexel University, Philadelphia, Pennsylvania 19104. *Received December 10, 1986*

Abstract: Self-diffusion coefficients of toluene, acetonitrile, chloroform, and dichloromethane in swollen 1-20% cross-linked polystyrene beads have been determined by application of a new model to magnetization-transfer ^{13}C NMR data for exchange of solvent in and out of the beads. The results agree closely with solvent self-diffusion coefficients in the same samples determined independently by the pulsed-gradient spin-echo NMR method. The new method also has been applied to self-diffusion of dichloromethane in macroporous polystyrene beads.

Self-diffusion coefficients of constituents of polymer solutions, plasticized polymers, micelles, microemulsions, and lyotropic and smectic liquid crystals have been determined by the pulsed-gradient spin-echo (PGSE) NMR method.[1-7] We report here a new method for determination of self-diffusion coefficients of solvents in polystyrene beads and in the pores of macroporous polystyrenes based on magnetization-transfer NMR (MT-NMR), and the application of the PGSE method to the same samples. Previously PGSE NMR experiments showed that the self-diffusion coefficients of toluene in cross-linked polystyrene beads were equal to those in toluene solutions of linear polystyrene containing the same weight fraction polymer as in the gel.[8]

The MT-NMR method is based on the observation that polystyrene beads packed into an NMR tube and swollen with solvent frequently show two peaks for each solvent carbon atom in their ^{13}C NMR spectra.[9-11] Those peaks can be assigned to solvent inside and outside the beads on the basis of the spin-lattice relaxation times (T_1) and on the basis of relative peak areas in spectra of samples that contain much more interstitial solvent than intraparticle solvent.[9] The rate of exchange of solvent between the two environments is of the same order of magnitude as the rate of spin-lattice relaxation and can be followed by selective inversion-recovery T_1 experiments. Nonlinear least-squares analysis of the data provides T_1's of the solvent in each environment and a first-order rate constant for exchange. Separate resonances for solvents and ions inside and outside of polymer beads have been reported earlier in both ^1H[12-19] and ^{13}C[9-11,20] NMR spectra.

* To whom correspondence should be addressed.
† Department of Chemistry, Oklahoma State University.
‡ Department of Physics, Oklahoma State University.
§ Drexel University. F.D.B. is now at the Department of Chemistry, University of Missouri—Rolla, Rolla, MO 65401.

(1) Stejskal, E. O.; Tanner, J. E. *J. Chem. Phys.* **1965**, *42*, 288.
(2) von Meerwall, E. D. *Adv. Polym. Sci.* **1983**, *54*, 1.
(3) Karger, J. *Adv. Colloid Interface Sci.* **1985**, *23*, 129.
(4) Stilbs, P. J. *Prog. NMR Spectros.* **1987**, *19*, 1.
(5) Cheever, E.; Blum, F. D.; Foster, K. R.; Mackay, R. A. *J. Colloid Interface Sci.* **1985**, *104*, 121.
(6) Blum, F. D.; Padmanabhan, A. S.; Mohebbi, R. *Langmuir* **1985**, *1*, 127.
(7) Blum, F. D. *Spectroscopy (Springfield, OR)* **1986**, *1*, 32.
(8) Pickup, S.; Blum, F. D.; Ford, W. T.; Periyasamy, M. *J. Am. Chem. Soc.* **1986**, *108*, 3987.
(9) Ford, W. T.; Periyasamy, M.; Spivey, H. O. *Macromolecules* **1984**, *17*, 2881.
(10) Ford, W. T.; Periyasamy, M.; Spivey, H. O.; Chandler, J. P. *J. Magn. Reson.* **1985**, *63*, 298.
(11) Periyasamy, M.; Ford, W. T. *React. Polym.* **1985**, *3*, 351.
(12) Gordon, J. E. *J. Phys. Chem.* **1962**, *66*, 1150.
(13) Doskocilova, D.; Schneider, B. *Macromolecules* **1972**, *5*, 125.
(14) Smith, W. B.; Strom, E. T.; Woessner, D. E. *J. Magn. Reson.* **1982**, *46*, 172.
(15) Creekmore, R. W.; Reilley, C. N. *Anal. Chem.* **1970**, *42*, 570.
(16) Creekmore, R. W.; Reilley, C. N. *Anal. Chem.* **1970**, *42*, 725.
(17) Frankel, L. S. *J. Phys. Chem.* **1971**, *75*, 1211.

0002-7863/87/1509-7276$01.50/0

Scheme I

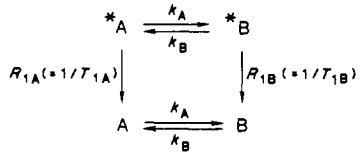

Rates of exchange of water in and out of ion-exchange resins have been determined by saturation-transfer ^{1}H NMR spectroscopy,[15,16] the continuous wave NMR predecessor of the pulsed magnetization-transfer method used here.

Experimental Section

Reagent grade solvents were used without further purification. Gel copolymer beads of styrene and divinylbenzene (Polysciences, 55% active) were prepared by a standard procedure.[21] Swollen gel bead sizes were measured microscopically and are reported in the figure captions as the volume-average diameter of 50 beads. Macroporous polymer beads were obtained from Rohm & Haas Co. All polymer beads were washed thoroughly with water, acetone, dichloromethane, and methanol and were dried at 60 °C under vacuum before use.

A typical sample for a MT-NMR experiment was prepared by placing the polymer beads in a 5-mm NMR tube, adding 0.5 g of dichloromethane which contained 4 mg of 4-hydroxy-2,2,6,6-tetramethylpiperidinyloxy free radical (4-hydroxy-TEMPO, Aldrich Chemical Co.), and allowing the beads to swell completely. Air bubbles were removed by centrifugation. Benzene-d_6 (15 wt % with respect to dichloromethane) was added to provide the spectrometer frequency lock signal. A vortex plug was inserted to the level of the polymer beads to minimize the amount of interstitial solvent.

^{13}C NMR spectra were obtained at 75.43 MHz at 23 °C with a Varian XL-300 spectrometer with a ^{1}H decoupling field ($\omega = \gamma H_2$) of 2400 Hz. Selective inversion of one of the two overlapping solvent signals was achieved with the DANTE[22] pulse sequence as the 180° pulse of an inversion–recovery experiment. In the complete pulse sequence $[D_1-(P_1-D_2)_n-D_3-\text{PW}-\text{acquisition}]$, n times P_1 equals a 180° pulse and PW is a nonselective 90° pulse. MT-NMR data sets consisted of 32 spectra, 16 D_3 values between the 180° and 90° pulses for each of the doublet peaks. A more complete description of the method has been published.[10]

The PGSE experiments used ^{1}H NMR at 90 MHz. The technique is described in detail elsewhere.[7,8]

Results

In a typical ^{13}C NMR spectrum of solvent and swollen gel beads there are two overlapping solvent peaks, due to solvent inside and outside the beads. The peaks at 75 MHz are broadened by chemical shift dispersions to 15–45 Hz wide at half-height. Sometimes they are resolved without the addition of shift reagents. In other cases the addition of a stable free radical is necessary to obtain resolved solvent peaks. The methyl carbon peaks of toluene and the cyano carbon peaks of acetonitrile were analyzed without shift reagent. The chloroform samples contained TEMPO, and the dichloromethane samples contained 4-hydroxy-TEMPO. Exchange of solvent between the two environments occurs on a time scale similar to that of spin-lattice relaxation and could be described by the mechanism of Scheme I, in which *A and *B are magnetically perturbed species outside and inside the beads that exchange sites with rate constants k_A and k_B and undergo spin–lattice relaxation with rate constants R_{1A} and R_{1B}. Plots of peak intensities vs delay time in selective inversion–recovery T_1 experiments show qualitatively transfer of magnetization from the selectively inverted site to the other site. Data from two complementary selective inversion–recovery experiments were analyzed simultaneously by the Marquardt nonlinear least-squares method to obtain the spin–lattice relaxation rate constants in the two sites and the rate constants for exchange between the two sites.

Table I. Comparison of Simulated Diffusion Curves with First-Order Exchange Rate Constants Calculated from MT-NMR Data

Figure[a]	T_{1A}, s	T_{1B}, s	k_A, s^{-1}	k_B, s^{-1}	$(k_A + k_B)$, s^{-1}	$D_i \times 10^{10}$, $m^2\ s^{-1}$	slope, s^{-1}
						19.6	2.07
2	2.5	3.0	0.94	0.71	1.65	17.0	1.67
						14.5	1.40
						6.0	0.68
3	1.85	1.10	0.29	0.32	0.61	5.2	0.61
						4.4	0.54
						3.8	0.61
4	39	6.8	0.19	0.35	0.54	3.3	0.55
						2.8	0.49
						12.1	1.49
5	3.2	3.9	0.54	0.69	1.23	10.5	1.20
						8.9	0.97
						6.5	0.84
6	3.2	2.4	0.34	0.40	0.74	5.7	0.74
						4.8	0.64
						4.2	0.62
7	5.6	2.5	0.23	0.32	0.55	3.7	0.55
						3.1	0.50
						18.0	0.73
8	1.75	1.75	0.30	0.35	0.65	16.0	0.66
						14.0	0.57
						17.3	1.04
9	1.77	1.47	0.42	0.52	0.94	15.0	0.93
						12.8	0.87
						16.0	1.55
10	1.44	1.16	0.60	0.55	1.15	13.9	1.21
						11.8	0.95
						2.7	1.40
11	15.0	6.6	0.50	0.65	1.15	2.4	1.15
						2.0	0.98
						2.3	1.96
12	15.0	6.1	0.73	1.10	1.83	2.0	1.83
						1.70	1.69

[a] Figure 4, acetonitrile in 10% cross-linked, 193-μm beads. Figure 5, dichloromethane in 6% cross-linked, 239-μm beads. Figure 6, dichloromethane in 10% cross-linked, 227-μm beads. Figure 7, dichloromethane in 20% cross-linked, 217-μm beads. Figure 8, dichloromethane in 424-μm XAD-1 beads. Figure 9, dichloromethane in 408-μm XAD-2 beads. Figure 10, dichloromethane in 305-μm XAD-4 beads. Figure 11, toluene in 10% cross-linked, 115-μm beads. Figure 12, toluene in 10% cross-linked, 83-μm beads.

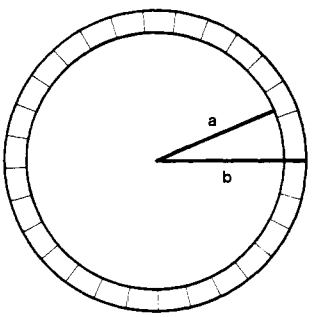

Figure 1. Geometrical model of bead surrounded by annular shell of solvent. In most experiments with beads tightly packed into solvent in an NMR tube the bead occupied about 0.6 of the volume.

Details of the analysis are given elsewhere.[10,23] Exchange rate constants k_A and k_B and spin–lattice relaxation times T_{1A} and T_{1B} are reported in Table I.

The exchange of solvent in and out of beads should be described by diffusion in spherical coordinates, not by a first-order chemical kinetic approach to equilibrium. The exchange rate constants in Table I are best fits to a theoretically incorrect mechanism. However, we demonstrate that in a limiting form this analysis does provide an estimate of the solvent self-diffusion coefficient inside the beads.

Calculation of self-diffusion coefficients from NMR exchange data requires application of Fick's law to a geometrical model for the sample. The problem of diffusion of an isotopically labeled species from a spherical bead into an infinite volume of sur-

(18) Frankel, L. S. *Anal. Chem.* **1971**, *43*, 1506.
(19) Narebska, A.; Streich, W. *Colloid Polym. J.* **1980**, *258*, 379.
(20) Sternlicht, H.; Kenyon, G. L.; Packer, E. L.; Sinclair, J. *J. Am. Chem. Soc.* **1971**, *93*, 199.
(21) Balakrishnan, T.; Lee, J.; Ford, W. T. *Macromol. Synth.*, in press.
(22) Morris, G. A.; Freeman, R. *J. Magn. Reson.* **1978**, *29*, 433.
(23) Led, J. J.; Gesmar, H. *J. Magn. Reson.* **1982**, *49*, 444.

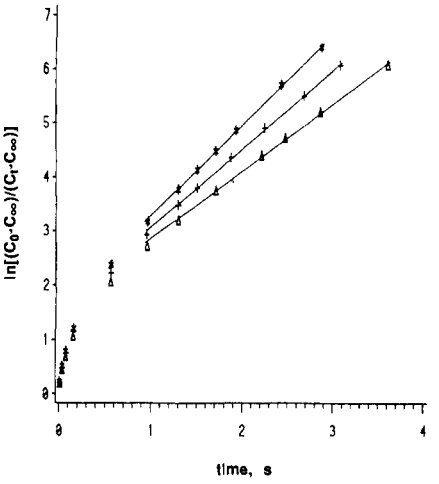

Figure 2. Simulated diffusion data for dichloromethane in 275-μm 1% cross-linked beads plotted as a first-order kinetic process. The best fit $\bar{D}_i$ (17.0×10^{-10} m^2 s^{-1}) has a slope of 1.67 s^{-1} in the linear region, which corresponds to $(k_A + k_B)$ = 1.65 s^{-1} calculated by kinetic treatment of MT-NMR data. The upper and lower straight lines correspond to $\bar{D}_i$ and $(k_A + k_B)$ values of 19.6×10^{-10} m^2 s^{-1} (2.07 s^{-1}) and 14.5×10^{-10} m^2 s^{-1} (1.40 s^{-1}), respectively.

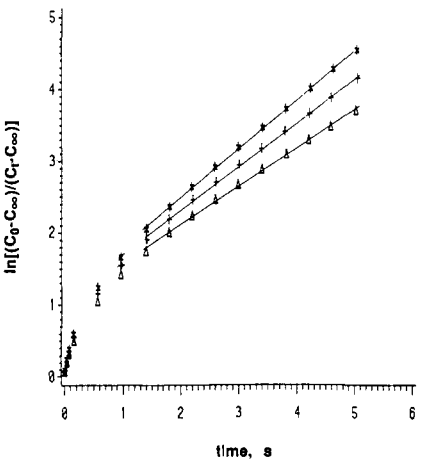

Figure 3. Simulated diffusion data for chloroform in 240-μm 10% cross-linked beads plotted as a first-order kinetic process. The best fit $\bar{D}_i$ (5.2×10^{-10} m^2 s^{-1}) has a slope in the linear region that corresponds to $(k_A + k_B)$ = 0.61 s^{-1} calculated by kinetic treatment of MT-NMR data. The upper and lower straight lines correspond to $\bar{D}_i$ and $(k_A + k_B)$ values of 6.0×10^{-10} m^2 s^{-1} (0.68 s^{-1}) and 4.4×10^{-10} m^2 s^{-1} (0.54 s^{-1}), respectively.

rounding liquid has a general solution,[24] but previously there was no known solution for the case of tightly packed spheres. We describe here qualitatively a model[25] for the diffusional exchange process that allows computer simulation of the diffusion of a magnetically (or isotopically) labeled species initially inside the bead to a random distribution inside and outside the bead at equilibrium. The model approximates the system as a spherical solvent-swollen polymer bead of radius a surrounded by an annular concentric sphere of solvent of radius b (Figure 1). The solvent is retained within the outer boundary b. A numerical, spherically symmetric solution to Fick's law is used to calculate distribution of a labeled species as a function of time and of distance from the center of the concentric spheres. Standard numerical methods[26] are employed in which the spatial node size is constrained by the time step size to ensure stability, and the label radial flux is constrained to be zero at the origin and at the radius b of the outer sphere. Initially the label is uniformly distributed only in the bead. At equilibrium the label is distributed such that it is an equal fraction of the solvent in both the bead and the annular shell. Four experimentally determined input parameters (1–4) and an estimate of the intraparticle self-diffusion coefficient of the solvent ($\bar{D}_i$) are required for each numerical simulation of the diffusion process. The four parameters are (1) the radius a of the bead, measured microscopically; (2) the relative amounts of solvent inside and outside the bead, measured by integration of the NMR spectra; (3) the radius b of the combined bead and annular sphere of solvent, calculated from the relative amounts of solvent in the two sites and the weight fraction solvent in the bead, which is measured by swelling experiments; and (4) the self-diffusion coefficient of bulk solvent ($\bar{D}_0$), determined independently by the PGSE method. The numerical calculation is carried out with a Fortran program on an IBM-7081D computer. The output is given as fractional approach to equilibrium distribution of the label as a function of time.

The proper description of the polymer beads in an NMR tube is amorphous packing of spheres with a distribution of bead radii, in which the ratio of radii of the largest and smallest beads is 1.67 for the 60/100-mesh fraction most often used (samples with swollen diameters in the 193-275-μm range). The concentric sphere model was chosen to make the numerical simulation of the diffusion tractable. We plan to address the geometrical problem elsewhere.[25]

Table II. Solvent Self-Diffusion Coefficients in Polystyrene Beads and in Bulk Liquid

solvent	% DVB	wt fr of polymer in beads	$\bar{D}_i \times 10^{10}$, m^2 s^{-1}		$\bar{D}_0 \times 10^{10}$, m^2 s^{-1}
			MT-NMR[a]	PGSE[b]	
toluene	10	0.602	2.12[c]	2.47	31.2
CH_3CN	10	0.788	3.3		49.8
$CHCl_3$	10	0.357	5.2		24.2[d]
CH_2Cl_2	1	0.165	17.0	20.7	36.5
CH_2Cl_2	6	0.359	10.5	8.9	36.5
CH_2Cl_2	10	0.467	5.7	6.4	36.5
CH_2Cl_2	20	0.586	3.7	3.7	36.5
CH_2Cl_2	XAD-1[e]	0.516	16.0		36.5
CH_2Cl_2	XAD-2[e]	0.582	15.0		36.5
CH_2Cl_2	XAD-4[e]	0.418	13.9		36.5

[a] 23 °C. [b] 25 °C. [c] Average of values of 2.00×10^{-10}, 2.37×10^{-10}, and 2.00×10^{-10} m^2 s^{-1} for particle diameters of 232, 115, and 83 μm. [d] 20 °C: Hardt, A. P.; Anderson, D. K.; Rathbun, R.; Mar, B. W.; Babb, A. L. *J. Phys. Chem.* **1959**, *63*, 2059. [e] Macroporous styrene–divinylbenzene copolymers from Rohm & Haas Co.

Since the MT-NMR analysis describes exchange of solvent between the two sites as a first-order chemical kinetic problem, the output from simulation of diffusion was plotted in first-order kinetic format as shown in Figures 2 and 3. The data points shown are representatives of a much larger set of output. The curves for simulated diffusion data show that diffusion redistributes the label early in the experiment much faster than first-order chemical kinetics would. However, in the time spans connected by the straight lines in Figures 2 and 3, the diffusion function is virtually superposable on the first-order chemical kinetic function. The three sets of data points in each figure are from three different trial values of the intraparticle self-diffusion coefficient $\bar{D}_i$. The center set of data points in the linear region has a slope that agrees within ±3% of the value of $(k_A + k_B)$, the sum of forward and reverse rate constants for first-order approach to chemical equilibrium calculated by application of the mechanism of Scheme I to the MT-NMR data. (A ln $[(c_0 - c_\infty)/(c_t - c_\infty)]$ vs time graph as in Figures 2 and 3 has a slope equal to the sum of the forward and reverse rate constants of a first-order reversible reaction.[27]) The upper and lower sets of data points in Figures 2 and 3 are from simulations of diffusion using intraparticle self-diffusion coefficients that differ from the best fit $\bar{D}_i$ of the center data set

(24) Helfferich, F. *Ion Exchange*; McGraw-Hill: New York, 1962; Chapter 6.
(25) Derivation and analysis of the model will be reported elsewhere: Ackerson, B. J.; Ford, W. T.; Periyasamy, M., manuscript in preparation.
(26) Holt, M. *Numerical Methods in Fluid Dynamics*; Springer-Verlag: Berlin, 1977.
(27) Frost, A. A.; Pearson, R. G. *Kinetics and Mechanism*, 2nd ed.; Wiley: New York, 1961; p 185.

by ±15%. The slopes of the upper and lower simulated diffusion data sets correspond with $(k_A + k_B)$ values that differ in 12 experiments by 9–24% from those calculated from MT-NMR data. Thus, even though this curve-fitting approach to the evaluation of self-diffusion coefficients of solvent inside the polymer beads is strictly empirical, we believe that it determines $\bar{D}_i$ to ±20%. In representative samples the self-diffusion coefficients have been determined also by the PGSE method (Table II). Differences between $\bar{D}_i$ values determined by the two methods range from 0 to 20%, well within the combined ranges of experimental errors of the two methods.

Since the first-order kinetic approximation appears to fit simulated diffusion only over a limited time domain (Figures 2 and 3), it would be appropriate to use NMR data from this time domain to calculate the exchange rate constants. For the experiment of Figure 2, use of NMR data only in the 1–4-s time domain (plus magnetization intensities at $t = 0$ and $t = \infty$ from least-squares analysis of the entire data set) gave a best fit $\bar{D}_i$ of 18.6×10^{-10} m^2 s^{-1} vs 17.0×10^{10} m^2 s^{-1} calculated from the complete data set. A similar analysis of data from a limited time domain of Figure 12 (Table I and Supplementary Material) gave $\bar{D}_i = 1.9 \times 10^{-10}$ m^2 s^{-1} vs 2.0×10^{-10} m^2 s^{-1} from the entire data set of Figure 12.

The need for tightly packed spheres in the model, rather than spheres in an infinite volume of liquid, was tested as follows. The best fit $\bar{D}_i$ from Figure 2, calculated with an experimentally determined bead packing fraction of 0.458, was used to simulate diffusion in cases of packing fractions of 0.1, 0.01, and 0.001. The slopes (rate constants) corresponding to Figure 2 for the smaller packing fractions were 0.61, 0.45, and 0.43 s^{-1}, respectively, whereas the best fit slope in Figure 2 is 1.65 s^{-1}. Similar application of the diffusion model with too small packing fractions to the experiment of Figure 3 also gave large variation in rate constants that did not agree with those calculated from MT-NMR data. Therefore, the experimental packing fraction is essential for the estimation of $\bar{D}_i$.

Results from application of the model to MT-NMR data obtained with a variety of swelling solvents and a variety of cross-linked polystyrene beads are in Table II. The empirical fits of simulated diffusion with first-order kinetics are in Figures 2–12[28] and Table I. Most experiments employed divinylbenzene–cross-linked polystyrene beads 150–250 μm in diameter before swelling. Application of the MT-NMR method with toluene in 10% cross-linked beads of three different diameters gave an average deviation of 8% from the $\bar{D}_i$ value in Table II, excellent agreement considering that the probable errors in MT-NMR exchange rate constants are ±15%. $\bar{D}_i$ values determined by the PGSE method were calculated from the echo intensities late in the decay curve, with a probable error of ±10%. In the case of dichloromethane two separate proton NMR peaks were observed in the PGSE spectra, and only the intensity of the peak due to solvent inside the beads was followed.

The MT-NMR method was applied also to intraparticle diffusion in the macroporous polystyrene adsorbents XAD-1, XAD-2, and XAD-4, in which most, but not all, of the solvent is in macropores rather than in the polymer network.

In principle, numerical solution of the diffusion model and the nonlinear least-squares analysis of MT-NMR data should be combined by modification of the Bloch equations for spin–lattice relaxation for diffusion between the two sites instead of first-order exchange between the two sites. We have tried this approach without least-squares analysis. A second simulation of the diffusion process was devised with simultaneous spin–lattice relaxation in the two sites using the same model. The input parameters were initial and final magnetization intensities in each site, spin–lattice relaxation rates in each site, bead radius, bead packing fraction, relative amounts of solvent in the two sites, and diffusion coefficients in the two sites, as in the first simulation method. The input parameters chosen initially were the magnetization intensities and relaxation rates calculated from the first-order kinetic analysis of the MT-NMR data. Only one data set from selective inversion at one site could be treated at one time. Even with substantial intuitive variation of the input initial magnetization intensities and relaxation rates, we were unable to fit satisfactorily an experimental data set of magnetization intensities in two sites as a function of time. However, the iterative least-squares procedure has not yet been applied to this more complex calculation. The full nonlinear least-squares minimization of complementary MT-NMR data sets by the Bloch equations modified for chemical exchange is needed for accurate determination of exchange rate constants in the usual MT-NMR kinetic measurement.[10,23] Simultaneous analysis of complementary data sets is likely to be needed also when the exchange process is described by diffusion rather than chemical kinetics.

(28) Figures 4–12 are available in microform.

Discussion

Previously the self-diffusion coefficient of toluene in polystyrene beads determined by the PGSE method was shown to decrease as the degree of swelling of the beads decreased. $\bar{D}_i$ of toluene in swollen beads correlated closely with $\bar{D}_i$ of toluene in polystyrene/toluene solutions having the same weight compositions as the gel beads.[8] The trend of decreasing $\bar{D}_i$ with increasing cross-linking and increasing weight fraction polystyrene for dichloromethane in the beads is shown in Table II. Of particular importance to the chemistry of solid-phase peptide synthesis and of polymer-supported reagents and catalysts, $\bar{D}_i$ for dichloromethane in the 1% cross-linked beads is reduced only by about a factor of 2 compared with bulk liquid. The greatest reduction in $\bar{D}_i$ inside the beads, a factor of 15, occurred with acetonitrile, the poorest swelling solvent, in the sample with the highest weight fraction of polymer.

The macroporous XAD-1, XAD-2, and XAD-4 beads differ from the other samples in that the dichloromethane resides both in permanent pores and in a slightly swollen polymer network. The percent cross-linking of the polymers increases and the median pore sizes decrease in the order XAD-1 (21 nm), XAD-2 (9 nm), and XAD-4 (5 nm).[29] Macroporous beads are of special interest as adsorbents, as catalyst supports, and as column packings for gel permeation chromatography. Since most of the solvent in each sample is in the macropores, the $\bar{D}_i$ values represent mainly pore diffusion. Even in XAD-4 the pore size is large with respect to molecular dimensions. One might expect $\bar{D}_i$ to decrease with decreasing pore size (XAD-1 > XAD-2 > XAD-4), but there is no clear trend in the data. Possibly with increased cross-linking there is also a trend of decreasing amount of solvent in the gel phase, such that there is a decreasing contribution to $\bar{D}_i$ from slow-diffusing solvent in the gel phase. Thus the sample with the largest pores, XAD-1, might have the largest pore diffusion coefficient but also the largest contribution from much slower diffusing solvent in the slightly swollen polymer network, whereas the sample with the smallest pores, XAD-4, might have the smallest pore diffusion coefficient but also the smallest contribution from solvent in the polymer network.

On a molecular level both the gel and the macroporous polystyrene beads are heterogeneous. The self-diffusion coefficients of solvents in the beads are averages over all local environments regardless of whether they are determined by the PGSE method or by curve-fitting of the diffusion model to MT-NMR data.

The MT-NMR and PGSE methods complement one another. The PGSE method is most readily applied to samples in which the diffusion distance during the experiment is small relative to the size of the particle. It can be used for $\bar{D}_i$ values as low as 10^{-11} m^2 s^{-1} in the polystyrene gel beads. (The limit is determined by T_2, not $\bar{D}_i$.) The MT-NMR method requires a heterogeneous sample with resolved NMR peaks from a species exchanging between the two sites. Exchange lifetimes from about 0.1 s to twice the T_1 in the faster relaxing site can be determined. Variation of the particle size permits determination of $\bar{D}_i$ in the approximate range of 10^{-9}–10^{-11} m^2 s^{-1}. Applications of the

(29) Gustafson, R. L.; Albright, R. L.; Heisler, J.; Lirio, J. A.; Reid, O. T., Jr. *Ind. Eng. Chem., Prod. Res. Dev.* **1968**, *7*, 107. Albright, R. L., personal communication.

MT-NMR method to diffusion in particles important in chromatography and in gel phase synthesis are in progress.

Acknowledgment. We thank the National Science Foundation for support through Grants DMR-8304251 (W.T.F.), DMR-8500704 (B.J.A.), and DMB-8603864 (to the Oklahoma State University Department of Chemistry for upgrade of the NMR spectrometer) and the donors of the Petroleum Research Fund, administered by the American Chemical Society, for support of the research of F.D.B. We thank M. P. Sudhakaran for help with Fortran programming.

Supplementary Material Available: Figures 4-12 showing simulated diffusion for the remainder of the experiments of Table I plotted as in Figures 2 and 3 (9 pages). Ordering information is given on any current masthead page.

Deuterium and Carbon-13 NMR of the Solid Polymorphism of Benzenehexoyl Hexa-*n*-hexanoate

E. Lifshitz,[†] D. Goldfarb,[†] S. Vega,[†] Z. Luz,*[†] and H. Zimmermann[‡]

Contribution from The Weizmann Institute of Science, Rehovot 76100, Israel, and Max-Planck-Institut fur Medizinische Forschung, 6900 Heidelberg, West Germany.
Received December 15, 1986

Abstract: Deuterium and carbon-13 NMR of specifically labeled benzenehexoyl hexa-*n*-hexanoate in the various solid-state phases are reported. The spectra exhibit dynamic line shapes which change discontinuously at the phase transitions. The results are interpreted in terms of sequential "melting" of the side chains on going from the low-temperature solid phases IV, III, etc., toward the liquid. In phase IV the molecules are very nearly static, except for fast rotation of the methyl groups about their C_3 axes. The results in phase III were quantitatively interpreted in terms of a two-site isomerization process involving simultaneous rotation by 95° about C_1-C_2 and transition from *gtg* to *g'g't* (or equivalently *g'tg'* to *ggt*) for the rest of the chain. The specific rate of this reaction at 0 °C is $\sim 10^5$ s^{-1}. In phase II additional chain isomerization processes set-in which were, however, not analyzed quantitatively. Further motional modes, involving reorientation of whole chains about their C^{ar}-O bonds, appear on going to phase I. In all solid phases the benzene ring remains static.

I. Introduction

Discotic mesogens are liquid crystalline compounds whose molecules consist of a flat central core to which several (usually six) aliphatic side chains are bonded via ethers, esters, or other linkages.[1,2] The orientational order of the central core in the liquid-crystalline phase is generally quite high, but the side chains are highly disordered.[3] Several of these discotic compounds were shown to undergo a succession of solid-solid transitions, as a function of temperature below the mesophase or normal liquid regions.[4-8] An example of this behavior is exhibited by homologues of the benzenehexoyl hexa-*n*-alkanoate series (hereafter referred to as BHA*n*, where *n* designates the number of carbons in each of the side chains, see Figure 1). Detailed thermodynamic measurements on the homologues with $n = 6$, 7, and 8 were recently published[4-7] and interpreted in terms of step-wise "melting" of the side chains. However, these measurements do not provide direct information on the nature of the melting process. In favorable cases this type of information may be obtained from ^{13}C or ^{2}H NMR of specifically labeled species, and in the present paper we present such a study for the BHA6 homologue. Although, in pure form, this compound does not exhibit a mesophase[9,10] the general pattern of its solid-solid transitions is similar to that of the $n = 7$ and 8 homologues which are mesogenic.

The phase diagram of isotopically normal BHA6 is given in the upper row of Table I. There are four solid phases labeled IV, III, II, and I with increasing temperature. The transitions between them are all first order and accompanied by large transition entropies. On the basis of thermodynamic and IR measurements it was speculated[5] that the phase transitions reflect the following "melting" sequence of the side chains: Starting from a rigid all-trans structure in phase IV, the transition to phase III is accompanied by the onset of methyl group rotations, in phase II methylenes 5 and 4 attain full disorder, and in phase I methylene 3 starts to reorient. According to this model, only in the liquid state do the rest of the chain carbons undergo complete conformational disorder (in addition to overall rotational and translational disorder). We show below that although the phase transitions are indeed associated with chain melting the details are entirely different.

Table I. Phase Transition Temperatures (K) of the Various BHA6 Isotopomers

	IV	III	II	I	iso
BHA6[a]	251.58	291.46	348.27	368.74	
BHA6-*2-d*	254.60	291.00	352.00	366.80	
BHA6-*3-d*	250.40	289.80	350.70	367.00	
BHA6-*4-d*	247.90	289.00	348.80	368.20	
BHA6-*5-d*	248.50	291.30	349.20	368.00	
BHA6-*6-d*	249.50	287.50	347.20	366.20	

[a] Transition temperature of the isotopically normal compound.

[†] The Weizmann Institute of Science.
[‡] Max-Planck-Institut fur Medizinische Forschung.

(1) Billard, J. In *Liquid Crystals of One and Two Dimensional Order*; Helfrich, W., Heppke, G., Eds.; Springer-Verlag: Berlin, 1980; p 383.
(2) Dubois, J. C.; Billard, J. In *Liquid Crystals and Ordered Fluids*; Griffin, A. C., Johnson, J. F., Eds.; Plenum: New York, 1984; Vol. 4, p 1043.
(3) Goldfarb, D.; Luz, Z.; Zimmermann, H. *Isr. J. Chem.* **1983**, *23*, 341. Luz, Z.; Goldfarb, D.; Zimmermann, H. In *Nuclear Magnetic Resonance of Liquid Crystals*; Emsley, J. W., Ed.; D. Reidel Publishing Co.: Dortrecht, Holland, 1985; p 343.
(4) Sorai, M.; Tsuji, K.; Suga, H.; Seki, S. *Mol. Cryst. Liq. Cryst.* **1980**, *59*, 33.
(5) Sorai, M.; Suga, H. *Mol. Cryst. Liq. Cryst.* **1981**, *73*, 47.
(6) Sorai, M.; Yoshioka, H.; Suga, H. *Mol. Cryst. Liq. Cryst.* **1982**, *84*, 39.
(7) Sorai, M. *Thermochim. Acta* **1985**, *88*, 1.
(8) Van Hecke, G. R.; Kaji, K.; Sorai, M. *Mol. Cryst. Liq. Cryst.* **1986**, *136*, 197.
(9) Chandrasekhar, S.; Sadashiva, B. K.; Suresh, K. A. *Praman* **1977**, *9*, 471.
(10) Chandrasekhar, S.; Sadashiva, B. K.; Suresh, K. A.; Madhusudana, N. V.; Kumar, S.; Shashidhar, R.; Venkatesh, G. *J. Phys. Colloque C3* **1979**, *40*, 3-20.

0002-7863/87/1509-7280$01.50/0